

T cell receptor engagement of peptide-major histocompatibility complex class I does not modify CD8 binding

David K. Cole^{a,*}, Steven M. Dunn^b, Malkit Sami^b, Jonathan M. Boulter^a,
Bent K. Jakobsen^b, Andrew K. Sewell^a

^a Department of Medical Biochemistry & Immunology, Henry Wellcome Building, Cardiff University,
School of Medicine, Heath Park, Cardiff, CF14 4XN, United Kingdom

^b Medigene UK Limited, 57C Milton Park, Abingdon, Oxon, OX14 4RX, United Kingdom

Received 9 November 2007; accepted 14 December 2007

Available online 19 February 2008

Abstract

Activation of cytotoxic T cells is initiated by engagement of the T-cell receptor (TCR) with peptide-major histocompatibility class I complexes (pMHCI). The CD8 co-receptor also binds to pMHCI, but at a distinct site, and allows the potential for tripartite TCR/pMHCI/CD8 interactions, which can increase T cell antigen sensitivity. There has been a substantial interest in the effect of the pMHCI/CD8 interaction upon TCR/pMHCI engagement, and several conflicting studies have examined this event, using the soluble extracellular domains of CD8 and the TCR, by surface plasmon resonance. However, the evidence to date suggests that the TCR engages cognate pMHCI before CD8 recruitment, so the question of whether TCR engagement alters CD8 binding is likely to be more relevant to the biological order of T cell antigen encounter. Here, we have examined the binding of CD8 to several variants of the HLA A2-restricted telomerase_{540–548} antigen (ILAKFLHWL) and the HLA A2-restricted NY-ESO-1_{157–165} antigen (SLLMWITQC) that bind to their cognate TCRs with distinct affinities and kinetics. These interactions represent a range of agonists that exhibit different CD8 dependency for activation of their respective T cells. By using engineered affinity enhanced TCRs to these ligands, which have extended off-rates of ~1 h compared to seconds for the wildtype TCRs, we have examined pMHCI/CD8 binding before and during TCR-engagement. Here we show that the binding of the extracellular domain of the TCR to pMHCI does not transmit structural changes to the pMHCI-CD8 binding site that would alter the subsequent pMHCI/CD8 interaction.

© 2007 Elsevier Ltd. All rights reserved.

Keywords: TCR; CD8-co-receptor; T cell; Antigen recognition; K_D ; Surface plasmon resonance

1. Introduction

Cytotoxic T lymphocyte (CTL) antigen recognition and CTL activation are mediated by T-cell receptor (TCR) engagement of peptide-major histocompatibility complex class I (pMHCI). However, the activities of the CD8 co-receptor (expressed mainly on MHC class I-restricted CTLs) (Cantor and Boyse, 1975) can increase T-cell antigen sensitivity, and aid activation (Janeway, 1992). The CD8 co-receptor binds to the same pMHCI complex as the TCR, but at a spatially distinct site from the TCR/pMHCI antigen-specific interaction (Gao et al., 1997; Janeway, 1992), enabling the possibility for tripartite

TCR/pMHCI/CD8 interactions to take place. This system of two receptors engaging one ligand to generate intracellular signal transduction is unique to T cells. Cooperative binding of the TCR and CD8 during pMHCI engagement may be an important mechanism by which T cell activation is achieved, and has therefore been the subject of many studies (Garcia et al., 1996; Wooldridge et al., 2005; Wyer et al., 1999).

Experiments using soluble pMHCI have determined that CD8 stabilizes the TCR/pMHCI interaction at the cell surface (Luescher et al., 1995; Wooldridge et al., 2005) by about two-fold and there has been considerable interest in the possibility that the binding of the extracellular domain of CD8 to pMHCI modifies the TCR binding site (Garcia et al., 1996; Wyer et al., 1999). The first study to examine whether the extracellular domains of the TCR and CD8 cooperate in binding pMHCI concluded that CD8 enhances formation of TCR/pMHCI complexes

* Corresponding author. Fax: +44 2920687007.
E-mail address: coledk@cf.ac.uk (D.K. Cole).

(Garcia et al., 1996). However, the surface plasmon resonance (SPR) data presented in this study exhibited characteristics consistent with the presence of protein aggregation (Wooldridge et al., 2005) and our own subsequent studies utilizing the same techniques have reached the opposite conclusion (Wyer et al., 1999). More recently, fluorescent resonance energy transfer (FRET) based examinations of the TCR/pMHCI/CD8 antigen recognition complex have shown that the TCR binds before CD8 (Yachi et al., 2006). This order of antigen engagement is likely to be important in ensuring that the specific interaction between the TCR and pMHCI dominates CTL recognition. Thus the question of whether TCR binding alters the binding site for CD8 is more relevant to T cell biology than the question that has been addressed previously of whether CD8 binding affects TCR engagement.

Here, we used a range of ligands known to exhibit the full spectrum of CD8-dependencies, from total CD8 dependence to near CD8 independence in order to elicit T cell activation, in order to study whether the engagement of pMHCI by the TCR affects subsequent CD8 binding. By utilizing engineered high affinity TCRs that bind to pMHCI with the same overall conformation as the wildtype TCRs, but with half-lives of ~1 h as opposed to a few seconds for the wildtype TCR/pMHCI interactions, we were able to use SPR to measure CD8 binding before and during TCR/pMHCI engagement in real time.

2. Materials and methods

2.1. Generation of expression plasmids

The HLA-A*0201 telomerase_{540–548} restricted wildtype TCR (Tel TCR), the HLA-A*0201 telomerase_{540–548} high affinity TCR (c13 TCR) and the HLA A*0201 NY-ESO-1_{157–165} restricted high affinity TCR (c49c50 TCR) α and β chains, the CD8 α chain and the HLA-A*0201 (A2), A*02402 (A24) (Cole et al., 2006) and B*0801 (B8) α chain and β 2m sequences were generated by PCR mutagenesis (Stratagene) and PCR cloning. All sequences were confirmed by automated DNA sequencing (Lark Technologies). The high affinity c13 TCR and c49c50 TCR were produced using a phage display library based on the HLA-A*0201 telomerase_{540–548} (ILAKFLHWL) antigen (A2 Tel) and the HLA A*0201-restricted NY-ESO-1_{157–165} (SLLMWITQC) antigen (A2 NY-ESO-1) respectively, the method of which has been previously reported (Li et al., 2005). The Tel TCR, the c13 TCR and the c49c50 TCR were constructed using a disulphide linked construct to produce the soluble domains (variable and constant) for both the α (residues 1–207) and β chains (residues 1–247) (Boulter et al., 2003; Garboczi et al., 1996). The A2, A24 (Cole et al., 2006) and B8 (Kjer-Nielsen et al., 2002) soluble heavy chain (residues 1–248) (α 1, α 2 and α 3 domains), tagged with a biotinylation sequence, and β 2m (residues 1–100) were also cloned and used to make the pMHCI complexes. For CD8, the α chain domain (residues 1–120) was cloned to make the CD8 $\alpha\alpha$ homodimer. The TCR α and β chains, CD8, the A2 α chain and β 2m sequences were inserted into separate pGMT7 expression plasmids under the control of the T7 promoter (Garboczi et al., 1996).

2.2. Protein expression, refolding and purification

BL21 Rosetta DE3 *E. coli* cells were used to produce the TCR α and β chains, the CD8 α chain and the A2, A24 and B8 heavy and β 2m chains in the form of inclusion bodies (IBs) using 0.5 mM IPTG to induce expression as described previously (Garboczi et al., 1996). For a 1 L refold, 30 mg of TCR α chain IBs were incubated at 37 °C for 15 min with 10 mM DTT and added to 1 L of cold refold buffer (50 mM TRIS pH 8.1, 2 mM EDTA, 2.5 M urea, 6 mM cysteamine hydrochloride and 4 mM cystamine). After 10–15 min, 30 mg of TCR β chain, incubated for 10–15 min at 37 °C with 10 mM DTT, was added. For a 1 L pMHCI refold, 30 mg of α chain was mixed with 30 mg of β 2m, 4 mg of synthetic peptide and 10 mM DTT at 37 °C for 15 min, which were then added to 1 L of cold refold buffer (50 mM TRIS pH 8.1, 2 mM EDTA, 400 mM L-arginine, 6 mM cysteamine hydrochloride and 4 mM cystamine). For the pMHCI/CD8 binding analysis before and during TCR/pMHCI engagement, three different A2 complexes were refolded with three different 9 mer peptides derived from the screening of a mutant peptide library based on the A2 Tel antigen. These included; A2 Tel, A2-ILGKFLHWL (A2 3G) and A2-ILAKYHWL (A2 5Y). The A2 NY-ESO-1 protein was also refolded for this analysis. Furthermore, we screened CD8 binding against a number of other pMHCI complexes in order to compare CD8 binding over a broad range of different ligands. These were as follows; A*0201-LLFGYPVYV (A2 Tax), A*2402-PYLFWLAAI (A24 EBV), A*0201-YLEPGPVTV (A2 GP100), A*0201-ELAGIGILTV (A2 Mel), A*0201-GILGFVFTL (A2 Flu) and B*0801-FLRGRAYGL (B8 EBNA). Refolding of TCR and pMHCI was performed at 4 °C for >1 h. Dialysis was carried out against 10 mM TRIS, pH 8.1 until the conductivity of the refolds was under 2000 μ S. The refolds were then filtered through a 0.45 μ M filter, ready for purification steps. The refolded TCR and pMHCI proteins were purified initially by ion exchange using a Poros 50HQTM column.

Refolding of CD8 was carried out as previously described (Cole et al., 2007b; Gao et al., 1998) with some modifications. For a 1 L refold, 60 mg of CD8 α chain IBs were incubated in 6 mL of 6 M guanidine buffer at 37 °C for 15 min with 10 mM DTT. The denatured IBs were then added to 1 L of cold refold buffer (100 mM TRIS-base, 76 mM TRIS-acid, 1 mM EDTA, 600 mM L-arginine, 6 mM cysteamine hydrochloride and 4 mM cystamine). The CD8 refold was then mixed at 4 °C for >1 h. Dialysis was carried out against 10 mM MES pH 6 until the conductivity of the refolds was under 2000 μ S. The refolds were then filtered through a 0.45 μ M filter, ready for purification steps. The CD8 protein was initially purified by cation exchange using 10 mM MES pH 6 as binding buffer and 10 mM MES pH6, 1 M NaCl as elution buffer, using a Poros50 HSTM column.

All of the soluble proteins (TCR, pMHCI and CD8) were then gel filtered into BIAcore buffer (10 mM HEPES pH 7.4, 150 mM NaCl, 3 mM EDTA and 0.005% (v/v) Surfactant P20), using a Superdex 200HRTM column. This step was implemented on the day of analysis, and concentration of the proteins was kept to a minimum in order to minimize protein aggregation. Proteins quality was analyzed by Coomassie-stained SDS-PAGE.

2.3. pMHCI biotinylation

Biotinylated pMHCI was prepared as previously described (Wyer et al., 1999).

2.4. SPR equilibrium analysis

The binding analysis was performed using a BIAcore 3000™ equipped with a CM5 sensor chip as previously reported (Wyer et al., 1999). Approximately 400–800 RUs of each pMHCI was coupled to the CM5 sensor chip via a biotin–streptavidin interaction to ensure the correct orientation of the pMHCI ligand. For the analysis, 10 serial dilutions of the Tel TCR (300–0.3 μM) were injected over the chip coupled pMHCI to test the Tel TCR binding affinity and kinetics to the A2 Tel variants at concentrations at least 10 times above and 10 times below the known K_D of the interaction. Secondly, 10 serial dilutions of CD8, at 500–0.5 μM , were injected over the chip coupled pMHCI. This was followed by a single injection of the high affinity c13 TCR, or c49c50 TCR, at $\sim 0.5 \mu\text{M}$. Due to the longer high lives of the high affinity TCRs (~ 1 h), this resulted in the formation of more stable TCR/pMHCI complex on the chip surface compared to wildtype TCR/pMHCI interactions. Following this injection, a further 10 serial dilutions of CD8 was immediately injected over the TCR/pMHCI complex. As a control, these steps were repeated independently using a buffer injection, and a pMHC class II (pMHCII)-restricted TCR (HA1.7) injection, between the two CD8 serial dilution injections. These controls were used in order to determine whether any observed effect on pMHCI/CD8 binding during TCR/pMHCI engagement was, in fact, due to the alternation of the CD8 binding domain of the pMHCI molecule in the TCR/pMHCI complex, or whether any differences were due pMHCI degradation after an extended period of experimentation. Results were analyzed using BIAevaluation 3.1™, Microsoft Excel™ and Origin 6.1™. The K_D values were calculated assuming 1:1 Langmuir binding ($AB = B \times AB_{\text{MAX}}/(K_D + B)$) and were plotted using a nonlinear curve fit ($y = (P_1x)/(P_2 + x)$).

2.5. SPR kinetic analysis

Experiments were carried out to determine the K_{on} and K_{off} values for the Tel TCR, the c13 TCR and the c49c50 TCR at 25 °C. For all kinetic experiments, approximately 300 RUs of pMHCI was coupled to the CM5 sensor chip surface. The Tel TCR was concentrated to 300 μM and 10 serial dilutions (300–0.3 μM) were injected onto the chip at 30 $\mu\text{L}/\text{min}$. The response was measured over a 45 s injection period with a 60 s dissociation period. In order to examine the binding of the c13 TCR and c49c50 TCR at a concentration identical to that used during the CD8 binding experiments, each TCR was used at a concentration of $\sim 0.5 \mu\text{M}$ and a single kinetic injection was carried out with a 120 s association period and a 90 min dissociation period. The K_{on} and K_{off} values were calculated assuming 1:1 Langmuir binding ($AB = B \times AB_{\text{MAX}}/(K_D + B)$) and the data were analyzed using a global fit algorithm (BIAevaluation™ 3.1).

2.6. SPR kinetic titration analysis

In order to more stringently examine the binding of the c13 TCR and c49c50 TCR at a greater range of concentrations, we used a new method for analyzing the kinetic parameters of high affinity interactions with long off-rates, utilizing state of the art BIAcore T100™ technology. The c13 TCR was analyzed at five concentrations ranging from 317 to 1.24 nM and the c49c50 TCR was analyzed at five concentrations ranging from 228 to 0.89 nM. These concentrations represent the greatest range we could accurately achieve around the K_D of each interaction. During the analysis, ~ 200 RUs of pMHC were immobilized onto the CM5 sensor chip surface. Each concentration of TCR was injected at a high flow rate of 45 $\mu\text{L}/\text{min}$ for a 240 s association period and a 120 s dissociation period. The final and highest concentration had a longer dissociation period of 600 s. A fast flow rate and a low amount of immobilized pMHC were used in order to limit association and dissociation mass transfer limitations as recommended by the experts at BIAcore™. The K_{on} and K_{off} values were calculated assuming 1:1 Langmuir binding ($AB = B \times AB_{\text{MAX}}/(K_D + B)$) and the data were analyzed using the kinetic titration analysis algorithm (BIAevaluation™ 3.1) (Karlsson et al., 2006).

2.7. Statistical analysis

A two-tailed Student *T*-test using equal variance (calculated using an *F*-test) was performed to analyze the statistical difference between the average K_D values for pMHCI/CD8 ($n = 5$) binding before and during TCR engagement ($n = 5$) using Microsoft Excel XP™. An identical statistical test was used to measure the difference between the pMHCI/CD8 binding before and during TCR engagement (Fig. 3) to the other wildtype pMHCI/CD8 interactions measured (Fig. 4).

3. Results and discussion

3.1. Wildtype and high affinity TCR binding to the A2 variants

It is well established that CTLs exhibit differential dependencies on the CD8 co-receptor in order to recognize cognate antigen (Gostick et al., 2007; Laugel et al., 2007; MacDonald et al., 1982). More recent studies indicate that CD8 can enhance antigen recognition by over a million-fold, and that CD8 is required for the recognition of all natural antigens presented at physiological levels (Holler and Kranz, 2003). Our own studies of the recognition of A2 Tel have identified a number of variants that bind to the Tel TCR with affinities both sides of the Tel TCR/A2 Tel interaction ($K_D = 34 \pm 2 \mu\text{M}$) (Cole et al., 2007a; Laugel et al., 2007). At one end of this spectrum, the A2 3G variant binds with an affinity over 10-fold higher than the wildtype peptide, while the range at the other end of the affinities are too low to measure reliably by SPR ($K_D < 500 \mu\text{M}$). For the purposes of this study we examined the A2 Tel, the A2 3G and the A2 5Y antigens, the last of which represents the weak-

est of the Tel TCR/A2 variant interactions where we were able to reliably measure the binding affinity and kinetics by SPR. These three peptides exhibit different potencies, from super-agonist through to weak agonist (Laugel et al., 2007) and also exhibit the full range of CD8-dependencies from being almost CD8-independent (A2 3G) through to exhibiting a complete dependency on the CD8 co-receptor for activation at all peptide concentrations (A2 5Y) (Laugel et al., 2007). These observations, made with the same TCR and ligands that are different at just a single amino acid position, seriously challenge the supposition that CD8-dependent and CD8-independent TCRs exhibit different docking orientations on the pMHC I binding platform (Buslepp et al., 2003).

In order to address whether soluble TCR/pMHC I binding affects the soluble pMHC I/CD8 interaction, we used two newly developed soluble high affinity TCRs. The c13 TCR, which has been affinity matured against A2 Tel (Purbhoo et al., 2007), and the c49c50 TCR, which has been affinity matured against A2 NY-ESO-1 (Dunn et al., 2006). These TCRs bind with affinities (K_D s) in the nM range, compared to K_D s in the μ M range for the wildtype TCRs, and have extended off-rates of ~ 1 h, compared to wildtype TCRs that have off-rates off a few seconds. The longer half-lives of these high affinity TCR/pMHC I interactions were sufficient to allow CD8 equilibrium binding experiments to be undertaken whilst the TCR was docked to pMHC I, thus enabling CD8 affinity measurements to be determined before and during TCR/pMHC I engagement.

SPR was used to determine the equilibrium binding constant (K_D) and the K_{on} and K_{off} values for the Tel TCR to three antigens that differ widely in their CD8-dependency (Fig. 1; Table 1a). The K_D values calculated from the kinetics ($K_{off}/K_{on} = K_D$) were virtually identical to the K_D values calculated from the equilibrium plots (data not shown). The Tel TCR bound to A2 Tel, A2 3G and A2 5Y with binding affinities of $K_D = 33 \mu\text{M}$, $K_D = 3 \mu\text{M}$, $K_D = 242 \mu\text{M}$, respectively and half-lives of 4.6, 9.9 and 2.2 s, respectively at 25 °C (Fig. 1, Table 1a). The wildtype TCR specific for the A2 NY-ESO-1 antigen (IG4 TCR), has previously been shown to bind to A2 NY-ESO-1 with a K_D of 13.3 μM and a half-life of 4.1 s (Table 1a) (Chen et al., 2005). These half-lives were not sufficient to enable examination of CD8 binding to pMHC I during TCR engagement.

In order measure CD8 binding to pMHC I during TCR engagement, we used the high affinity c13 TCR, which bound to A2 Tel, 3G and 5Y variants with a higher affinity ($K_D = 3$, 3.3 and 16.7 nM, respectively) and a longer half-life (55, 31 and

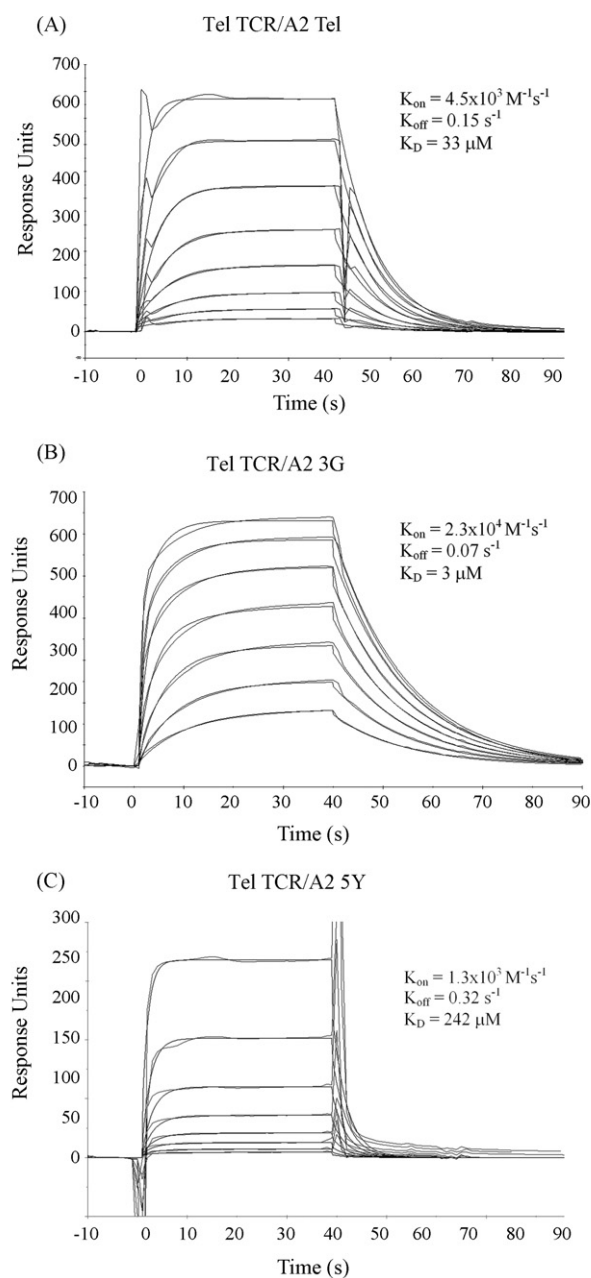


Fig. 1. Kinetic binding analysis of the Tel TCR to the A2 variants at 25 °C. (A–C) The binding of the Tel TCR to the A2 variants confirms correct native folding of the proteins. Ten serial dilutions of concentrated TCR were injected at 30 $\mu\text{l}/\text{min}$ for 45 s association periods and 60 s dissociation periods (seven or eight injections are shown). The solid lines for each binding response were calculated assuming 1:1 Langmuir binding ($AB = B \times AB_{\text{MAX}} / (K_D + B)$) and the data was analyzed using a global fit algorithm (BIAevaluationTM 3.1) to calculate K_{on} and K_{off} values.

Table 1a

Tel TCR kinetic, K_D and equilibrium binding values for the A2 variants and for the IG4 TCR against A2 NY-ESO-1 (previously published (Chen et al., 2005))

pMHC I epitope	Peptide Sequence	K_{on} ($\text{M}^{-1} \text{s}^{-1}$)	K_{off} (s^{-1})	Half-life (s)	K_D (μM)
Tel	ILAKFLHWL	4.5×10^3	0.15	4.6	33 ± 1.8
3G	ILGKFLHWL	2.3×10^4	0.07	9.9	3 ± 0.2
5Y	ILAKYLHWL	1.3×10^3	0.32	2.2	242 ± 20
NY-ESO-1	SLLMWITQC	1.2×10^4	0.17	4.1	13.3 ± 0.4

Standard deviation is shown for the K_D values ($n=4$).

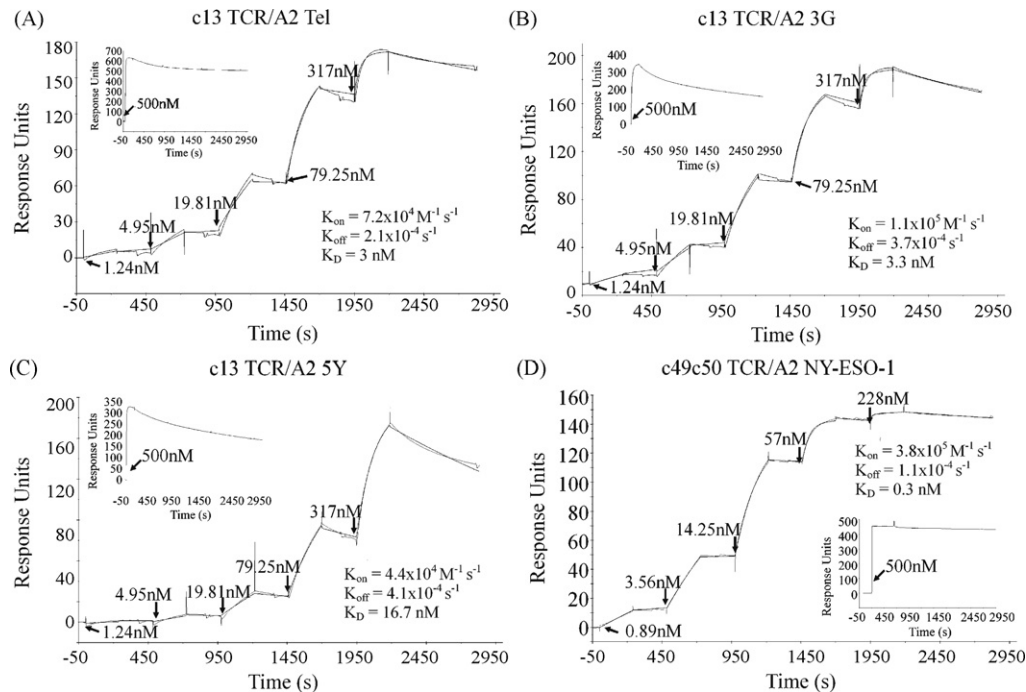


Fig. 2. Kinetic titration analysis of the c13 TCR and the c49c50 TCR to the A2 variants at 25 °C. (A–C) The c13 TCR kinetic binding responses to (A) A2 Tel, (B) A2 3G and (C) A2 5Y. (D) The c49c50 TCR kinetic binding response to A2 NY-ESO-1. The K_{off} of the c13 TCR and the c49c50 TCR to their specific ligands was of sufficient duration to allow equilibrium binding analysis of CD8 whilst the pMHC1 on the chip was still coupled to the high affinity TCRs. The main plot shows the kinetic titration injection series for each TCR. The solid line for each binding response was calculated assuming 1:1 Langmuir binding ($AB = B \times AB_{MAX} / (K_D + B)$) and the data was analyzed using a kinetic titration analysis algorithm (BIAevaluation™ 3.1) to calculate K_{on} and K_{off} values. The smaller panel in each window shows single kinetic injections of the c13 TCR and the c49c50 TCR, at a flow rate 30 $\mu\text{L}/\text{min}$, and a concentration of ~ 500 nM. For these analyses, a 120 s association period and 90 min dissociation period were used. The solid line for each binding response was calculated assuming 1:1 Langmuir binding ($AB = B \times AB_{MAX} / (K_D + B)$) and the data was analyzed using a global fit algorithm (BIAevaluation™ 3.1) to calculate K_{on} and K_{off} values.

Table 1b

c13 TCR kinetic binding values for the A2 Tel variants and c49c50 TCR kinetic binding values for A2 NY-ESO-1

pMHC1 epitope	Peptide sequence	K_{on} ($\text{M}^{-1} \text{s}^{-1}$)	K_{off} (s^{-1})	Half-life (min)	K_D (nM)
A2 Tel	ILAKFLHWL	7.2×10^4	2.1×10^{-4}	55	3
A2 3G	ILGKFLHWL	1.1×10^5	3.7×10^{-4}	31	3.3
A2 5Y	ILAKYLHWL	4.4×10^4	4.1×10^{-4}	28	16.7
A2 NY-ESO-1	SLLMWITQC	3.8×10^5	1.1×10^{-4}	105	0.3

28 min, respectively) than the Tel TCR (Fig. 2, Table 1b), and the c49c50 TCR that bound to A2 NY-ESO-1 stronger than for the 1G4 TCR, with a K_D of 0.3 nM and a longer half-life of 105 min (Fig. 2, Table 1b). These data were calculated by using both kinetic titration analysis, and a single kinetic injection of each TCR. Both of these analyses produced virtually identical results (data shown is from the kinetic titration analysis). These vastly extended half-lives for the high affinity TCR/pMHC1 interactions enabled complete saturation of pMHC1 with TCR during the CD8 equilibrium binding experiments. The increased affinity of the c13 TCR and the c49c50 TCR meant that they could be utilized at lower concentrations than the wild type TCRs, and a concentration of ~ 0.5 μM was sufficient to completely saturate all of the pMHC1 bound to the chip surface, as observed by an R_{max} within 90% of the number of RUs of immobilized pMHC1 (Fig. 2).

3.2. CD8 binding to pMHC1 before and during TCR engagement

Equilibrium binding experiments were used to determine the affinity of CD8 to each of the A2 variants before and after c13 TCR and c49c50 TCR engagement (Fig. 3; Table 2a). The binding affinity of CD8 to the A2 Tel variants, before TCR engagement, ranged from K_D s of 132–183 μM , with an average K_D of 149 μM . The binding affinity of CD8 to the A2 NY-ESO-1 antigen before TCR engagement was $K_D = 125$ μM . These values fall within the previously published values for CD8 binding (Cole et al., 2007b; Garcia et al., 1996; Kern et al., 1999; Wyer et al., 1999). The binding of CD8 to the c13 TCR engaged A2 Tel variants ranged between of 141–191 μM , with an average K_D of 159 μM . The binding affinity of CD8 to the c49c50 TCR engaged A2 NY-ESO-1 antigen was $K_D = 131$ μM . The statisti-

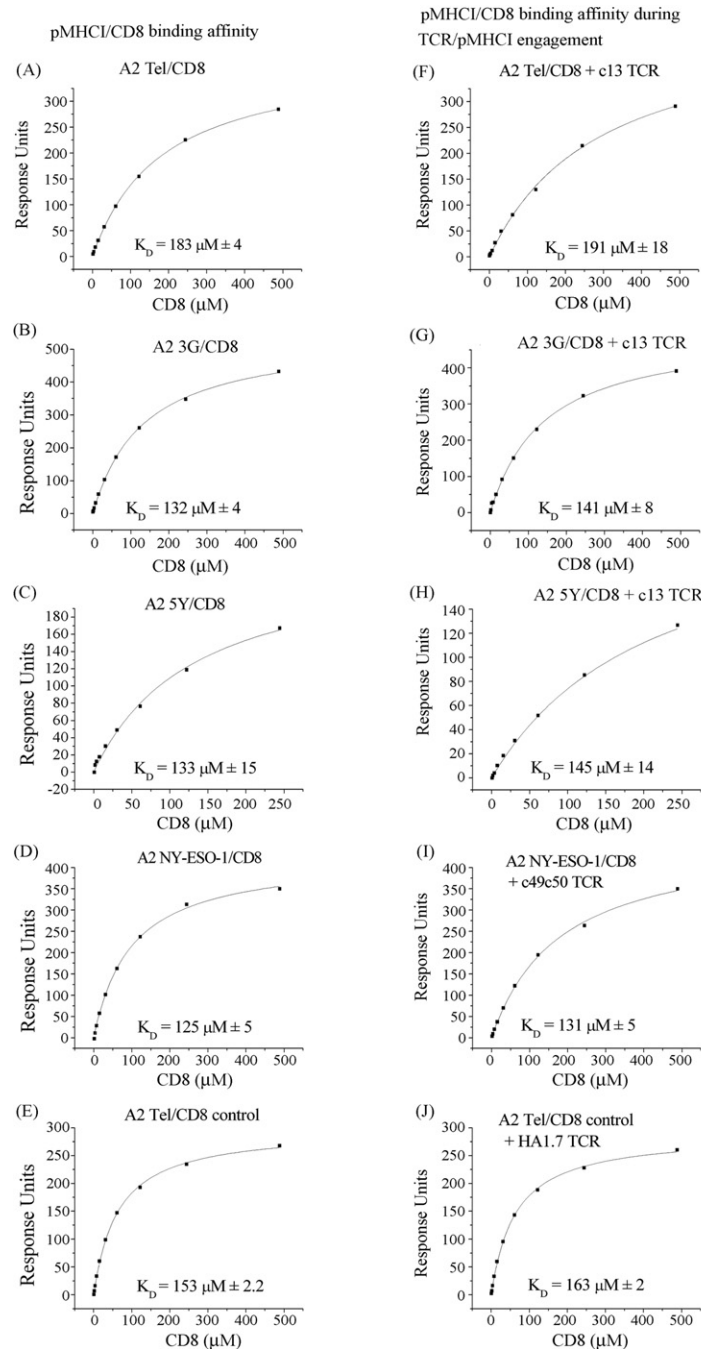


Fig. 3. Equilibrium binding analysis of CD8 to the A2 variants before and during TCR/pMHC engagement at 25 °C. (A–D) CD8 equilibrium binding responses to all of the A2 variants were within the normal CD8 binding range (120–200 μM). (E) CD8 equilibrium binding to A2 Tel as an independent control. (F–H) CD8 equilibrium binding responses to each of the A2 variants during c13 TCR engagement. (I) CD8 equilibrium binding responses to A2 NY-ESO-1 during c49c50 TCR engagement. (J) CD8 equilibrium binding responses to the A2 Tel control after the injection of a pMHC class II specific TCR (HA1.7). The duration of each CD8 equilibrium binding experiment was ~10 min, during which the pMHC coupled to the chip was completely saturated with the c13 TCR, or the c49c50 TCR. The affinities recorded for pMHC/CD8 before and during TCR/pMHC engagement were not significantly different ($P=0.66$). Ten serial dilutions were carried out for each equilibrium experiment. The average response for each concentration was plotted with standard deviation ($n=4$). The equilibrium dissociation constant (K_D) values were calculated assuming 1:1 Langmuir binding ($AB = B \times AB_{MAX}/(K_D + B)$) and were plotted using a nonlinear curve fit ($y = (P_1x)/(P_2 + x)$).

cal difference between CD8 binding to the A2 variants before and during c13 TCR and c49c50 TCR binding was measured using a two tailed T -test with equal variance. This analysis suggested there was no significant difference between pMHC/CD8

binding before and during TCR/pMHC engagement ($P=0.66$) and the difference was within the experimental error. Although statistically insignificant, a consistent decrease in CD8 affinity was observed during TCR docking for all of the A2 variants

Table 2a
CD8 equilibrium binding values for the A2 variants pre- and during high affinity TCR engagement

pMHCI epitope	A2/CD8 K_D (μ M)	A2/CD8 + c13 TCR K_D (μ M)
A2 Tel	183 \pm 4	191 \pm 18
A2 3G	132 \pm 4	141 \pm 8
A2 5Y	133 \pm 15	145 \pm 14
A2 NY-ESO-1	125 \pm 5	131 \pm 5
<i>F</i> -test	1	Same variance
<i>T</i> -test	0.66	<i>P</i> -value

Standard deviation is shown for the K_D values ($n = 4$).

Table 2b
Control equilibrium binding experiment for the pMHCI/CD8 interaction before and during TCR engagement

pMHCI Epitope	A2/CD8 K_D (μ M)	A2/CD8 + control TCR K_D (μ M)
A2 Tel	153 \pm 2.2	163 \pm 2

pMHCI/CD8 binding was measured before and after a pMHC class II specific TCR (HA1.7) was injected over the chip. Standard deviation is shown for the K_D values ($n = 4$).

Table 3
CD8 equilibrium binding values to five pMHCI antigens

pMHCI epitope	CD8 affinity (μ M)
A*0201 Tax (LLFGYPVYV)	160 \pm 8.7
A*2402 EBV (PYLFWLAAI)	142 \pm 4.5
A*0201 GP100 (YLEPGPVTV)	144 \pm 3.9
A*0201 Mel A (ELAGIGILTV)	127 \pm 3.7
B*0801 EBNA (FLRGRAYGL)	135 \pm 8.6
A*0201 Flu (GILGFVFTL)	172 \pm 11.6

Standard deviation is shown for the K_D values ($n = 3$).

(Table 2a). In order to test whether this was due to an effect of TCR-docking, the experiment was repeated using a pMHC class II restricted TCR that did not bind to A2 Tel or A2 NY-ESO-1 (HA1.7 TCR). The same small decrease in affinity was observed for this (Fig. 3E and J; Table 2b) and other control conditions (data not shown). Therefore, this statistically insignificant decrease in CD8 binding affinity to pMHCI before and during TCR/pMHCI binding is unlikely to be an effect of TCR docking to pMHCI. The small difference observed during the experiments is most likely due to pMHCI instability over the time course of the experiment at 25 °C. This would create a larger degree of conformation diversity of bound pMHCI during later CD8 injections, thereby decreasing rate of association, and therefore reducing the observed binding affinity of CD8.

To further analyze the binding affinity of CD8 to pMHCI and to confirm that CD8 bound to the A2 variants within the normal range, we measured this interaction using A2 Tax, A2 GP100, A2 Mel, A24 EBV, B8 EBNA and A2 Flu (Fig. 4, Table 3). The CD8 binding affinity ranged between $K_D = 127$ – 172μ M, with an average response of $K_D = 147 \mu$ M. A two-tailed student *T*-test with equal variance analysis showed no significant difference between CD8 binding to these other pMHCI molecules, and those recorded for the pMHCI/CD8 binding before ($P = 0.8$) and during TCR/pMHCI docking ($P = 0.7$).

3.3. Structural analysis of TCR binding affects on the CD8 binding site of pMHCI

The binding sites for TCR and CD8 on pMHCI are spatially distinct. Thus, the only way the binding of the soluble extracellular domain of the TCR can alter pMHCI/CD8 engagement would be to transmit a structural change to the pMHCI CD8 binding site. In order to gain a structural perspective of the events occurring around the pMHCI α 3 CD8 binding loop (residues 223–227) during TCR/pMHCI docking, we compared the conformation of this region using the crystal structures of free pMHCI and TCR/pMHCI complexes. Although unlikely, we first considered the possibility that differences in the mode of pMHCI binding for the high affinity TCRs might not lead to any potential structural rearrangement in the CD8 binding region of pMHCI that would occur during a wildtype TCR/pMHCI interaction. In order to investigate this, we compared the co-crystal structures of the 1G4 TCR and the c49c50 TCR complexed to the A2 NY-ESO-1 antigen. Our previous structural analyses of the 1G4 TCR (Chen et al., 2005) and the c49c50 TCR (Dunn et al., 2006) complexed to this antigen exclude the possibility of different modes of binding for the wildtype and high affinity TCRs (Sami et al., 2007). Fig. 5A shows a superposition of the 1G4 TCR/A2 NY-ESO-1 and the c49c50 TCR/A2 NY-ESO-1 structures. In both cases, the TCRs contact the A2 NY-ESO-1 antigen in an identical overall conformation, with the TCRs binding approximately diagonally to the pMHCI surface. The CDR-loops of the TCRs also contact the pMHCI surface in an identical manner, with the CDR3-loops contacting mainly the antigenic peptide, and the CDR1 and CDR2-loops contacting mainly the surface of the MHCI molecule (Fig. 5B). This analysis confirmed that the higher affinity interaction observed between the c49c50 TCR and A2 NY-ESO-1 was due to the formation of a few new specific interactions between residues in the α and β CDR2-loops of the TCR and the MHCI surface, rather than a major conformational rearrangement (Dunn et al., 2006). These differences in binding between the c49c50 TCR and the 1G4 TCR to A2 NY-ESO-1 had no significant structural effect on the pMHCI α 3 CD8 binding loop of the pMHCI molecule (Fig. 5C) (Chen et al., 2005).

In order to test whether our data was consistent with other TCR/pMHCI structures, we compared the structure of the CD8 binding site in A2 Tax, uncomplexed and complexed to the A6 TCR (Garboczi et al., 1996; Saper et al., 1991), and the structure of the CD8 binding site of B8 EBNA, bound and unbound to the LC13 TCR (Fig. 5D) (Kjer-Nielsen et al., 2002; Kjer-Nielsen et al., 2003). In both of these pMHCI molecules, where the structure of pMHCI complexed and uncomplexed to TCR has been determined, we observed a small degree of flexibility in the C α backbone of residues either side of the MHC α 3 CD8 binding loop, but the overall conformation of the loop remained virtually identical (Fig. 5D). Although the events on the surface of the cell may not be identical to those represented in crystal structures, these observations support our findings that the binding of soluble CD8 to pMHCI is unaffected by soluble TCR/pMHCI docking.

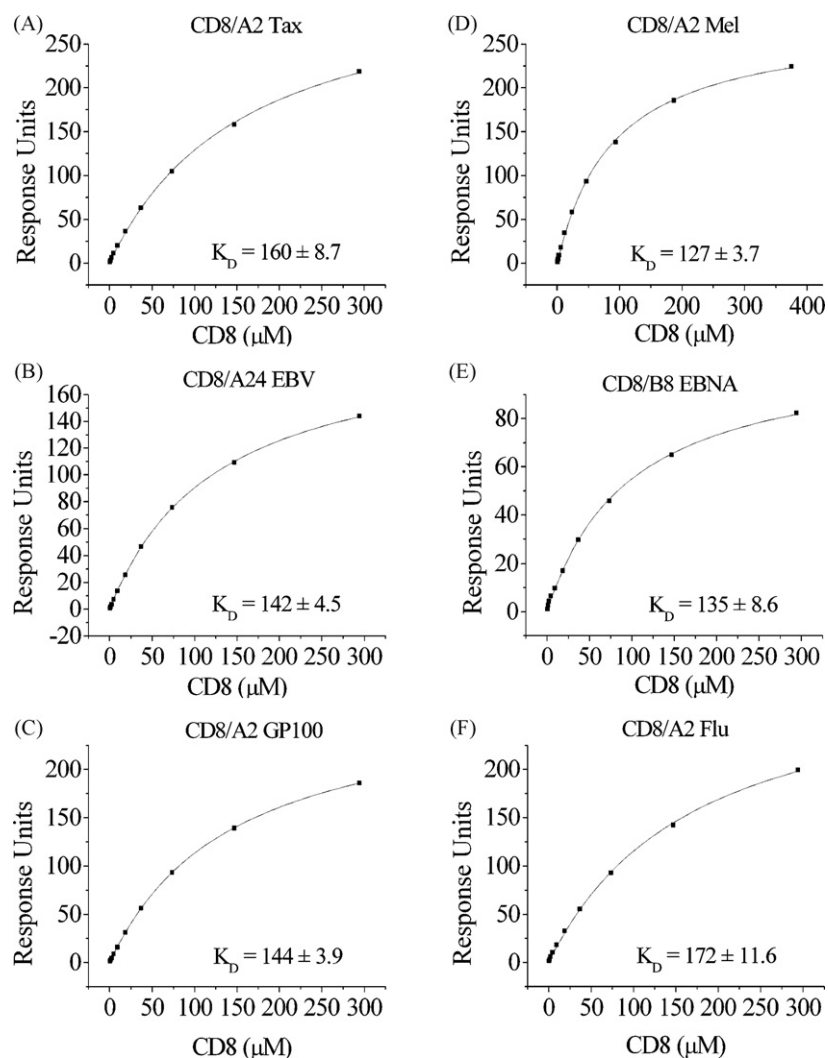


Fig. 4. Equilibrium binding analysis of CD8 to the pMHC variants at 25 °C. (A) A2 Tax/CD8, (B) A24 EBV/CD8, (C) A2 GP100/CD8, (D) A2 Mel/CD8, (E) B8 EBNA/CD8 and (F) A2 Flu/CD8. The average binding affinity ($K_D = 147 \mu\text{M}$) was not significantly different to the average K_D recorded for CD8 binding to the A2 variants before ($P=0.8$) and during ($P=0.7$) TCR engagement to pMHC. Ten serial dilutions were carried out for each equilibrium experiment. The average response for each concentration is plotted with standard deviation ($n=3$). The equilibrium dissociation constant (K_D) values were calculated assuming 1:1 Langmuir binding ($AB = B \times AB_{\text{MAX}}/(K_D + B)$) and were plotted using a nonlinear curve fit ($y = (P_1x)/(P_2 + x)$).

3.4. Conclusions

Previously, the effect of pMHC/CD8 docking upon TCR/pMHC engagement has been investigated in a number of studies, the conclusions of which remain disparate (Garcia et al., 1996; Wyer et al., 1999). However, recent FRET experiments indicate that the TCR binds to pMHC before CD8 (Yachi et al., 2006), an observation which is consistent with the more extensively studied CD4+T helper cell system, in which the TCR has been shown to bind to pMHC class II before the engagement of the CD4 coreceptor (Hampl et al., 1997; Madrenas et al., 1997). Therefore, the question of whether the initial binding of the TCR to pMHC affects the subsequent engagement of the pMHC by CD8 may be more relevant. This study is the first direct real-time analysis, using SPR, of CD8 binding affinity to pMHC before and during TCR engagement. We show that TCR binding to pMHC does not

affect the subsequent binding of CD8. Our use of high affinity TCRs with a half-life of ~ 1 h has enabled us to perform independent CD8 binding experiments during TCR/pMHC engagement. These data suggest that the cooperation observed between the TCR and CD8 at the cell surface during antigen engagement (Wooldridge et al., 2005) is not a consequence of structural alterations in the pMHC after docking to the TCR, which would enhance the binding of CD8 to the TCR/pMHC complex. Our observations are further supported by the available crystal structures of unbound pMHC and TCR/pMHC complexes (Garboczi et al., 1996; Kjer-Nielsen et al., 2002; Kjer-Nielsen et al., 2003; Madden et al., 1993). From our analysis, it is clear that there are no significant conformational changes in the $\text{C}\alpha$ backbone of the MHC $\alpha 3$ CD8 binding loop, which constitutes the main contact area for CD8 binding (Fig. 5c and d). We therefore conclude that the co-engagement of the soluble extracellular domain of CD8 to

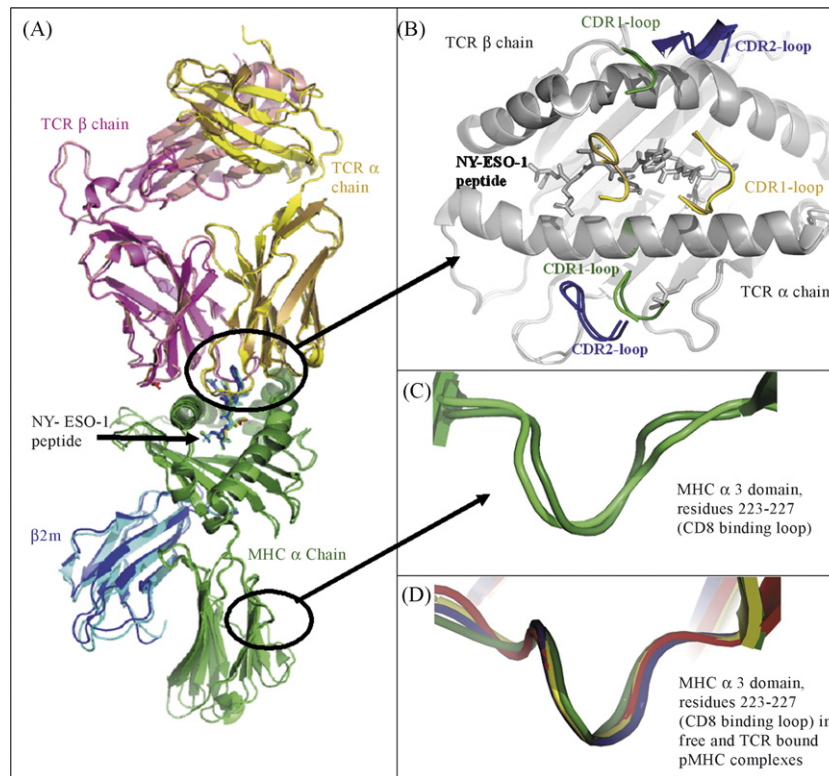


Fig. 5. A structural investigation of the effect of TCR/pMHC engagement on the CD8 binding domain of pMHC. (A) The 1G4 TCR (pink and yellow cartoon) complexed to A2-NY-ESO-1 (green and cyan cartoon with the NY-ESO-1 peptide shown at sticks) superposed to the c49c50 TCR (magenta and sand cartoon) complexed to A2 NY-ESO-1 (dark green and blue with the NY-ESO-1 peptide shown at sticks). The overall conformation of both complexes in the superposition is virtually identical. (B) The 1G4 TCR CDR1 (green), CDR2 (blue) and CDR3-loop (yellow) superposed with the c49c50 TCR CDR1 (dark green), CDR2 (dark blue) and CDR3-loop (sand) orientation over the surface of the A2 NY-ESO-1 molecule. The conformation of the CDR-loops is remarkably similar in both complexes. (C) A superposition of the A2 NY-ESO-1 $\alpha 3$ domain, residues 223–227 which constitutes the main pMHC/CD8 binding region, from the 1G4 TCR/A2 NY-ESO-1 complex (green) and the c49c50 TCR/A2 NY-ESO-1 complex (dark green). There are no large differences in the conformation of this region of the pMHC molecule. (D) Superposition of the MHC $\alpha 3$ domain, residues 223–227, of A2 Tax (yellow), A2 Tax complexed to the A6 TCR (green), B8 EBNA (blue) and B8 EBNA complexed to the LC13 TCR (red). It is evident in this superposition that the CD8 binding region of the pMHC molecule remains virtually unaltered in the free pMHC and the complexed TCR/pMHC structures.

pMHC is independent of, and unaffected by, the TCR/pMHC interaction.

Acknowledgements

We wish to thank Alan Bennett, Nikolai Lissin, Ruth Moysey, Nathaniel Liddy, Emma Baston, Brian Cameron, Penio Todorov, Yi Li and Annelise Vuidepot for their involvement in making TCR, MHC and CD8 constructs available for this study.

J.M.B. is supported by an RCUK academic fellowship. A.K.S. was a Wellcome Trust Senior Fellow. D.K.C. is supported by a Wellcome Trust VIP grant.

The authors claim no financial conflict of interest.

References

- Boulter, J.M., Glick, M., Todorov, P.T., Baston, E., Sami, M., Rizkallah, P., Jakobsen, B.K., 2003. Stable, soluble T-cell receptor molecules for crystallization and therapeutics. *Protein Eng.* 16, 707–711.
- Buslepp, J., Wang, H., Biddison, W.E., Appella, E., Collins, E.J., 2003. A correlation between TCR V alpha docking on MHC and CD8 dependence: implications for T cell selection. *Immunity* 19, 595–606.
- Cantor, H., Boyse, E.A., 1975. Functional subclasses of T-lymphocytes bearing different Ly antigens. I. The generation of functionally distinct T-cell subclasses is a differentiative process independent of antigen. *J. Exp. Med.* 141, 1376–1389.
- Chen, J.L., Stewart-Jones, G., Bossi, G., Lissin, N.M., Wooldridge, L., Choi, E.M., Held, G., Dunbar, P.R., Eshouf, R.M., Sami, M., Boulter, J.M., Rizkallah, P., Renner, C., Sewell, A., van der Merwe, P.A., Jakobsen, B.K., Griffiths, G., Jones, E.Y., Cerundolo, V., 2005. Structural and kinetic basis for heightened immunogenicity of T cell vaccines. *J. Exp. Med.* 201, 1243–1255.
- Cole, D.K., Pumphrey, N.J., Boulter, J.M., Sami, M., Bell, J.I., Gostick, E., Price, D.A., Gao, G.F., Sewell, A.K., Jakobsen, B.K., 2007a. Human TCR-binding affinity is governed by MHC class restriction. *J. Immunol.* 178, 5727–5734.
- Cole, D.K., Rizkallah, P.J., Boulter, J.M., Sami, M., Vuidepot, A.L., Glick, M., Gao, F., Bell, J.I., Jakobsen, B.K., Gao, G.F., 2007b. Computational design and crystal structure of an enhanced affinity mutant human CD8 alphaalpha coreceptor. *Proteins* 67, 65–74.
- Cole, D.K., Rizkallah, P.J., Gao, F., Watson, N.I., Boulter, J.M., Bell, J.I., Sami, M., Gao, G.F., Jakobsen, B.K., 2006. Crystal structure of HLA-A*2402 complexed with a telomerase peptide. *Eur. J. Immunol.* 36, 170–179.
- Dunn, S.M., Rizkallah, P.J., Baston, E., Mahon, T., Cameron, B., Moysey, R., Gao, F., Sami, M., Boulter, J., Li, Y., Jakobsen, B.K., 2006. Directed evolution of human T cell receptor CDR2 residues by phage display dramatically enhances affinity for cognate peptide-MHC without increasing apparent cross-reactivity. *Protein Sci.* 15, 710–721.
- Gao, G.F., Gerth, U.C., Wyer, J.R., Willcox, B.E., O'Callaghan, C.A., Zhang, Z., Jones, E.Y., Bell, J.I., Jakobsen, B.K., 1998. Assembly and crystallization

- of the complex between the human T cell coreceptor CD8alpha homodimer and HLA-A2. *Protein Sci.* 7, 1245–1249.
- Gao, G.F., Tormo, J., Gerth, U.C., Wyer, J.R., McMichael, A.J., Stuart, D.I., Bell, J.I., Jones, E.Y., Jakobsen, B.K., 1997. Crystal structure of the complex between human CD8alpha(alpha) and HLA-A2. *Nature* 387, 630–634.
- Garboczi, D.N., Ghosh, P., Utz, U., Fan, Q.R., Biddison, W.E., Wiley, D.C., 1996. Structure of the complex between human T-cell receptor, viral peptide and HLA-A2. *Nature* 384, 134–141.
- Garcia, K.C., Scott, C.A., Brunmark, A., Carbone, F.R., Peterson, P.A., Wilson, I.A., Teyton, L., 1996. CD8 enhances formation of stable T-cell receptor/MHC class I molecule complexes. *Nature* 384, 577–581.
- Gostick, E., Cole, D.K., Hutchinson, S.L., Wooldridge, L., Tafuro, S., Laugel, B., Lissina, A., Oxenius, A., Boulter, J.M., Price, D.A., Sewell, A.K., 2007. Functional and biophysical characterization of an HLA-A*6801-restricted HIV-specific T cell receptor. *Eur. J. Immunol.* 37, 479–486.
- Hanpl, J., Chien, Y.H., Davis, M.M., 1997. CD4 augments the response of a T cell to agonist but not to antagonist ligands. *Immunity* 7, 379–385.
- Holler, P.D., Kranz, D.M., 2003. Quantitative analysis of the contribution of TCR/pepMHC affinity and CD8 to T cell activation. *Immunity* 18, 255–264.
- Janeway Jr., C.A., 1992. The T cell receptor as a multicomponent signalling machine: CD4/CD8 coreceptors and CD45 in T cell activation. *Annu. Rev. Immunol.* 10, 645–674.
- Karlsson, R., Katsamba, P.S., Nordin, H., Pol, E., Myszka, D.G., 2006. Analyzing a kinetic titration series using affinity biosensors. *Anal. Biochem.* 349, 136–147.
- Kern, P., Hussey, R.E., Spoerl, R., Reinherz, E.L., Chang, H.C., 1999. Expression, purification, and functional analysis of murine ectodomain fragments of CD8alphaalpha and CD8alphabeta dimers. *J. Biol. Chem.* 274, 27237–27243.
- Kjer-Nielsen, L., Clements, C.S., Brooks, A.G., Purcell, A.W., Fontes, M.R., McCluskey, J., Rossjohn, J., 2002. The structure of HLA-B8 complexed to an immunodominant viral determinant: peptide-induced conformational changes and a mode of MHC class I dimerization. *J. Immunol.* 169, 5153–5160.
- Kjer-Nielsen, L., Clements, C.S., Purcell, A.W., Brooks, A.G., Whisstock, J.C., Burrows, S.R., McCluskey, J., Rossjohn, J., 2003. A structural basis for the selection of dominant alphabeta T cell receptors in antiviral immunity. *Immunity* 18, 53–64.
- Laugel, B., van den Berg, H.A., Gostick, E., Cole, D.K., Wooldridge, L., Boulter, J.M., Milicic, A., Price, D.A., Sewell, A.K., 2007. Different T cell receptor affinity thresholds and CD8 coreceptor dependency govern cytotoxic T lymphocyte activation and tetramer binding properties. *J. Biol. Chem.* 282, 23799–23810.
- Li, Y., Moysey, R., Molloy, P.E., Vuidepot, A.L., Mahon, T., Baston, E., Dunn, S., Liddy, N., Jacob, J., Jakobsen, B.K., Boulter, J.M., 2005. Directed evolution of human T-cell receptors with picomolar affinities by phage display. *Nat. Biotechnol.* 23, 349–354.
- Luescher, I.F., Vivier, E., Layer, A., Mahiou, J., Godeau, F., Malissen, B., Romero, P., 1995. CD8 modulation of T-cell antigen receptor–ligand interactions on living cytotoxic T lymphocytes. *Nature* 373, 353–356.
- MacDonald, H.R., Glasebrook, A.L., Cerottini, J.C., 1982. Clonal heterogeneity in the functional requirement for Lyt-2/3 molecules on cytolytic T lymphocytes: analysis by antibody blocking and selective trypsinization. *J. Exp. Med.* 156, 1711–1722.
- Madden, D.R., Garboczi, D.N., Wiley, D.C., 1993. The antigenic identity of peptide-MHC complexes: a comparison of the conformations of five viral peptides presented by HLA-A2. *Cell* 75, 693–708.
- Madrenas, J., Chau, L.A., Smith, J., Bluestone, J.A., Germain, R.N., 1997. The efficiency of CD4 recruitment to ligand-engaged TCR controls the agonist/partial agonist properties of peptide-MHC molecule ligands. *J. Exp. Med.* 185, 219–229.
- Purbhoo, M.A., Li, Y., Sutton, D.H., Brewer, J.E., Gostick, E., Bossi, G., Laugel, B., Moysey, R., Baston, E., Liddy, N., Cameron, B., Bennett, A.D., Ashfield, R., Milicic, A., Price, D.A., Classon, B.J., Sewell, A.K., Jakobsen, B.K., 2007. The HLA A*0201-restricted hTERT540-548 peptide is not detected on tumor cells by a CTL clone or a high-affinity T-cell receptor. *Mol. Cancer Ther.* 6, 2081–2091.
- Sami, M., Rizkallah, P.J., Dunn, S., Molloy, P., Moysey, R., Vuidepot, A., Baston, E., Todorov, P., Li, Y., Gao, F., Boulter, J.M., Jakobsen, B.K., 2007. Crystal structures of high affinity human T-cell receptors bound to peptide major histocompatibility complex reveal native diagonal binding geometry. *Protein. Eng. Des. Sel.* 20, 397–403.
- Saper, M.A., Bjorkman, P.J., Wiley, D.C., 1991. Refined structure of the human histocompatibility antigen HLA-A2 at 2.6 Å resolution. *J. Mol. Biol.* 219, 277–319.
- Wooldridge, L., van den Berg, H.A., Glick, M., Gostick, E., Laugel, B., Hutchinson, S.L., Milicic, A., Brenchley, J.M., Douek, D.C., Price, D.A., Sewell, A.K., 2005. Interaction between the CD8 coreceptor and major histocompatibility complex class I stabilizes T cell receptor–antigen complexes at the cell surface. *J. Biol. Chem.* 280, 27491–27501.
- Wyer, J.R., Willcox, B.E., Gao, G.F., Gerth, U.C., Davis, S.J., Bell, J.I., van der Merwe, P.A., Jakobsen, B.K., 1999. T cell receptor and coreceptor CD8 alphaalpha bind peptide-MHC independently and with distinct kinetics. *Immunity* 10, 219–225.
- Yachi, P.P., Ampudia, J., Zal, T., Gascoigne, N.R., 2006. Altered peptide ligands induce delayed CD8-T cell receptor interaction—a role for CD8 in distinguishing antigen quality. *Immunity* 25, 203–211.